This is an open access article published under a Creative Commons Non-Commercial No Derivative Works (CC-BY-NC-ND) Attribution License, which permits copying and redistribution of the article, and creation of adaptations, all for non-commercial purposes.

ACS AUTHORCHOICE

JACS
JOURNAL OF THE AMERICAN CHEMICAL SOCIETY

pubs.acs.org/JACS

Article

Long-Lived Charge-Transfer State from B−N Frustrated Lewis Pairs Enchained in Supramolecular Copolymers

Beatrice Adelizzi,[#] Pongphak Chidchob,[#] Naoki Tanaka, Brigitte A. G. Lamers, Stefan C. J. Meskers, Soichiro Ogi, Anja R. A. Palmans, Shigehiro Yamaguchi,* and E. W. Meijer*

Cite This: J. Am. Chem. Soc. 2020, 142, 16681−16689

Read Online

ACCESS | Metrics & More | Article Recommendations | Supporting Information

ABSTRACT: The field of supramolecular polymers is rapidly expanding; however, the exploitation of these systems as functional materials is still elusive. To become competitive, supramolecular polymers must display microstructural order and the emergence of new properties upon copolymerization. To tackle this, a greater understanding of the relationship between monomers' design and polymer microstructure is required as well as a set of functional monomers that efficiently interact with one another to synergistically generate new properties upon copolymerization. Here, we present the first implementation of frustrated Lewis pairs into supramolecular copolymers. Two supramolecular copolymers based on π-conjugated *O*-bridged triphenylborane and two different triphenylamines display the formation of B−N pairs within the supramolecular chain. The remarkably long lifetime and the circularly polarized nature of the resulting photoluminescence emission highlight the possibility to obtain an intermolecular B−N charge transfer. These results are proposed to be the consequences of the enchainment of B−N frustrated Lewis pairs within 1D supramolecular aggregates. Although it is challenging to obtain a precise molecular picture of the copolymer microstructure, the formation of random blocklike copolymers could be deduced from a combination of optical spectroscopic techniques and theoretical simulation.

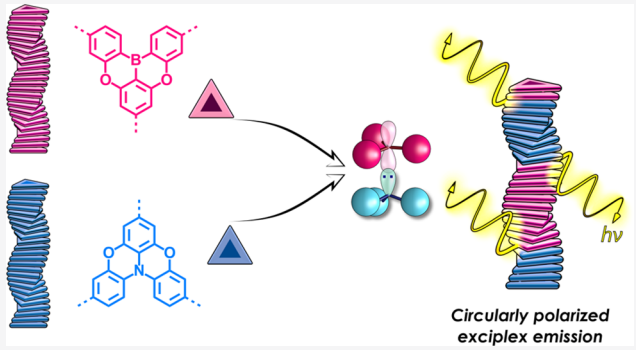

INTRODUCTION

Growing interest in the field of multicomponent supramolecular polymers stimulates research activities aimed to create new systems with precise microstructures and emerging properties. With the development of refined analytical, microscopic, and theoretical techniques, the field is currently establishing a systematic approach to characterize and control supramolecular copolymerizations. In past years, supramolecular copolymers with defined microstructures, such as alternating,[1,2] periodic,[3,4] and block,[5−10] have been reported. Each architecture has been obtained by finely tuning both the noncovalent interactions between different monomers and the balance between kinetic and thermodynamic control. The results achieved so far have laid the foundation of the field, but at the same time, predicting the resulting supramolecular architecture from the complex monomers' molecular structure remains a formidable challenge. Nevertheless, achieving emerging functions from supramolecular copolymers is of fundamental importance to unlock unforeseen possibilities and applications.

In this regard, frustrated Lewis pairs (FLP) represent a fascinating research field as their potential in a broad range of applications is expanding. FLPs are noncovalent adducts formed between a Lewis acid and a Lewis base that, because of their steric congestion, cannot create a covalent dative adduct.[11] Typical FLPs are based on highly Lewis acidic fluorinated triarylboranes and bulky triarylphosphines[11] or amines[12] as Lewis bases. The unique properties of FLPs are mainly exploited for metal-free catalysis[13−16] and, to a lesser extent, applied to optoelectronics[17−19] and responsive materials.[20,21] However, apart from a few examples of FLPs enchained in polymeric chains,[21] the use of these noncovalent adducts is currently confined to dimeric units. Developing a system that incorporates multiple FLPs into a larger ordered supramolecular assembly could be a promising approach for expanding the potentials of FLP-based materials. As supported by theoretical studies,[19] we envision that supramolecular systems bearing FLPs based on π-conjugated B and N compounds possess unexplored optoelectrical properties. As B−N FLPs have already shown great performances as organic light-emitting diodes,[17] the microstructural organization

Received: June 27, 2020
Published: September 3, 2020

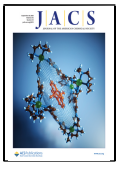

ACS Publications

© 2020 American Chemical Society

https://dx.doi.org/10.1021/jacs.0c06921
J. Am. Chem. Soc. 2020, 142, 16681−16689

achieved by supramolecular assembly will ensure long-range order, further improving their performances.[22,23]

Here, we report on the implementation of FLPs units into the classic design of supramolecular monomers for the development of FLP-based supramolecular copolymers. Our two groups joined forces as one has ample experience in the aggregation of nitrogen-centered C_3-symmetrical discotic molecules[24,25] and the other has studied in great detail the properties of boron-centered bridged disc-shaped molecules.[26,27] Our investigation sets out by exploring the possibility of converting FLPs based on B−N dimers into 1D supramolecular copolymers featuring B−N interactions as one of the noncovalent forces that defines the microstructure of the copolymer. With two sets of supramolecular copolymers (composed of the same B-based monomer but different N-based monomers), we present the first example of enchained FLPs in supramolecular polymers. We discovered that these copolymers exhibit long-lived, circularly polarized intermolecular charge transfer (CT) emission, which we believe holds great potential for supramolecular optoelectronics. The 1D electronic communication between FLP donors and acceptors could be an efficient driving force to realize an organic superconductor.[28]

RESULTS AND DISCUSSION

Design and Synthesis. The molecular designs of both B and N cores are inspired by classic triphenylborane−triphenylamine frustrated Lewis pairs. However, classic boron-based Lewis acids (i.e., triphenylborane and tris(pentafluorophenyl)-borane) are highly reactive and not stable in air. Thus, we opted for a partially *O*-bridged triphenylborane (***S*-B1**) whose electron-rich environment and structural rigidity impart higher stability to the boron center when compared to those of nonbridged analogues.[26,27,29] Bridged triarylboranes have been recently introduced as a new class of stable, organic electronic materials by one of us.[26,30] On the basis of the design of ***S*-B1**, two N cores were synthesized: (i) an analogous partially *O*-bridged triphenylamine, ***S*-N1**, and (ii) a triphenylamine core, ***S*-N2** and **a-N2**. Such cores have already demonstrated their potential as optoelectronic[31] and supramolecular materials.[32−34]

To impart directionality, we modified the peripheries of each core to accommodate three amide units as H-bonding supramolecular motifs. Each amide bears a gallic wedge functionalized with either chiral (*S*)-3,7-dimethyloctyl (***S*-B1**, ***S*-N1**, ***S*-N2**) or achiral *n*-octyl (**a-N2**) side chains to provide solubility in organic solvents (Scheme 1).

All monomers were synthesized via Suzuki cross-coupling reactions between a 3-fold brominated core, which was synthesized as previously reported,[35,36] with three boronate-ester functionalized peripheral wedges (Schemes S1−S4).[26] The solubilizing chains were synthesized via EDC-activated amide coupling between a gallic acid bearing three alkyl chains and 4-aminophenylboronic acid pinacol ester (Scheme S3). All monomers were obtained in high purity after purification and fully characterized by ^{1}H NMR, ^{13}C NMR, infrared spectroscopy and mass spectrometry (see Supporting Information for more details).

B- and N-Based Supramolecular Homopolymerization. Before investigating the copolymerization, we studied the individual assembly of B and N monomers via spectroscopic measurements in dilute apolar conditions (30 μM in decalin). The presence of chiral groups in ***S*-B1**, ***S*-N1**, and ***S*-N2** biases

Scheme 1. Chemical Structures of B and N Supramolecular Monomers[a]

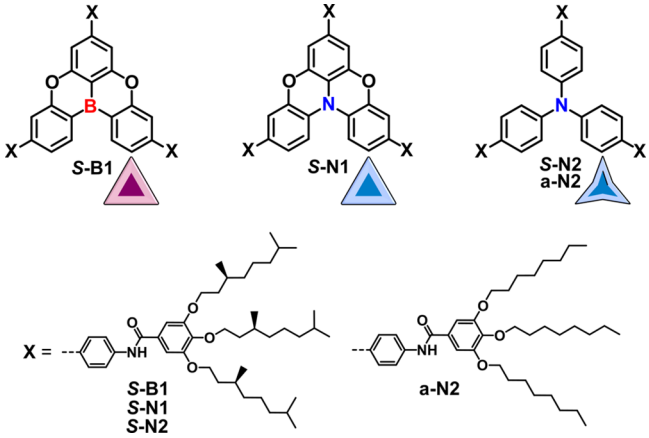

[a]***S*-B1** and ***S*-N1** have an *O*-bridged core that imparts higher rigidity and electron density to the core's atom compared to those of the triphenylamine of ***S*-N2** and **a-N2**. All the monomers' cores are functionalized with three peripheral gallic amides functionalized with either (*S*)-3,7-dimethyloctyl chains (***S*-B1**, ***S*-N1**, and ***S*-N2**) or *n*-octyl chains (**a-N2**).

the preferred helicity of the resulting supramolecular polymers (**poly(*S*-B1)**, **poly(*S*-N1)**, and **poly(*S*-N2)**), as observed by circular dichroism (CD). At 20 °C, all chiral supramolecular polymers display a negative Cotton effect at λ = 403 nm for **poly(*S*-B1)**, 441 nm for **poly(*S*−N1)**, and 370 nm for **poly(*S*-N2)** (Figure 1a,c,e).

Each supramolecular polymerization process was analyzed via variable-temperature (VT) UV−vis and CD spectroscopy (Figure 1, Figure S1) by slow cooling monomerically dissolved solutions from 100 to 20 °C at a cooling rate of 0.3 °C min^{-1}. Upon slow cooling, the supramolecular polymerization occurs as indicated by the increase in intensity of the CD bands and confirmed by the corresponding transitions in the UV−vis spectra (Figure S1). The bathochromic shift of the *O*-bridged monomers (***S*-B1** and ***S*-N1**) is in contrast with the hypsochromic shift detected for ***S*-N2**. This divergence is indicative of differences in the structural organization of the three supramolecular polymers (Figure S1). CD and UV−vis cooling curves—recorded by monitoring local maxima as a function of temperature—show nonsigmoidal transitions for all three systems. From VT-CD measurements, we identified the elongation temperatures (T_e) of each polymer as 78, 55, and 48 °C for **poly(*S*-B1)**, **poly(*S*-N1)**, and **poly(*S*-N2)** at 30 μM, respectively (Figure 1b,d,f and Figure S1). The sharp transitions are indicative of a cooperative nucleation−elongation growth of the supramolecular polymers consistent with these processes being driven by the formation of an intermolecular hydrogen-bonding network. The presence of a hydrogen-bonded network was further corroborated by infrared measurements (Figure S2).

Van't Hoff analyses on the three homopolymers (Figure S3) display comparable enthalpies of elongations (ΔH_e), suggesting that the diversity in the aggregation's behavior originates from the differences in entropy (ΔS_e) and enthalpy of nucleation (ΔH_n) rather than from that of elongation. We attributed these differences to the trigonal planar character of the boron core,[26,30,35,37] in contrast to a slightly twisted structure of the amine core, and to its electron-deficient

https://dx.doi.org/10.1021/jacs.0c06921
J. Am. Chem. Soc. 2020, 142, 16681−16689

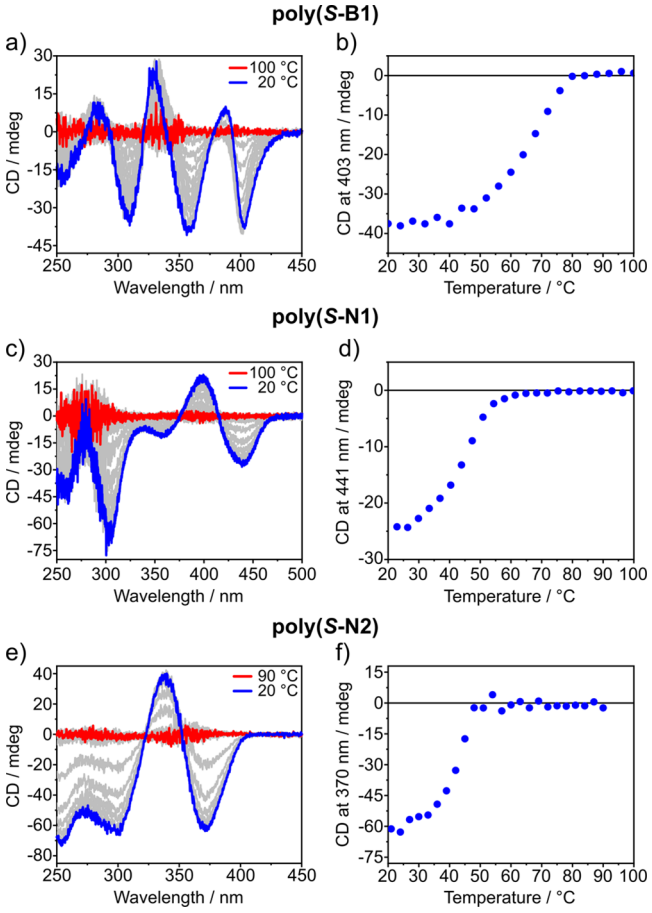

Figure 1. Supramolecular homopolymerization. VT-CD spectra of (a) **poly(*S*-B1)**, (c) **poly(*S*-N1)**, and (e) **poly(*S*-N2)** obtained via slow cooling from 100 or 90 °C (red lines) to 20 °C (blue lines) with 5 °C interval (gray lines). CD cooling curves of (b) **poly(*S*-B1)**, (d) **poly(*S*-N1)**, and (f) **poly(*S*-N2)**. Measurements were performed in decalin at c = 30 μM with a cooling rate of 0.3 °C min^{-1}.

character compared to the comparatively electron-rich nitrogen cores.[38,39] In addition, the lower conformational freedom of ***S*-N1** leads to polymers with higher T_e values (at equal concentration) than the ones based on the unbridged analogue ***S*-N2**.

Photophysical Study of B- and N-Based Supramolecular Homopolymers and Copolymers. The photoluminescence of a molecule strongly depends on the environment of the fluorophore and is therefore highly diagnostic for studying supramolecular (co)polymerizations. VT-photoluminescence measurements on all homopolymers reveal quenching of fluorescence accompanied by a red shift of the emission maximum (Figure S4). Upon cooling and polymerization, the monomers' bright emission in the far violet is replaced by the dimmed violet-blue emission of the related supramolecular aggregates (λ_{em} = 450, 470, and 410 nm for **poly(*S*-B1)**, **poly(*S*-N1)**, and **poly(*S*-N2)**, respectively; Figure 2 and Figures S4 and S5).

The high sensitivity of photoluminescence was further exploited to evaluate the formation of possible B−N interactions within a mixed supramolecular copolymer. The formation of FLPs between a π-conjugated donor (in this case, N) and acceptor (in this case, B) could result in charge-transfer (CT) processes in the ground and/or excited states.[17,40,41] Supramolecular copolymerizations were thus performed by

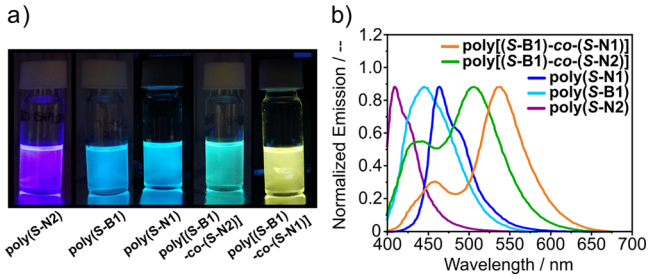

Figure 2. Photoluminescence properties. (a) A view of the emission of supramolecular homopolymers and copolymers under a long-wavelength UV lamp and (b) their emission spectra (λ_{exc} = 387 nm). Homopolymers **poly(*S*-N2)** (purple line), **poly(*S*-B1)** (light blue line), and **poly(*S*-N1)** (blue line) display violet-blue emission, while the copolymers **poly[(*S*-B1)-*co*-(*S*-N1)]** (orange line) and **poly[(*S*-B1)-*co*-(*S*-N1)]** (green line) display red-shifted emissions. Measurements were performed at 20 °C in decalin at c_{tot} = 30 μM (equimolar ratio of each monomer was used for copolymers).

mixing **poly(*S*-B1)** with an equimolar amount of either **poly(*S*-N1)** or **poly(*S*-N2)**, giving **poly[(*S*-B1)-*co*-(*S*-N1)]** and **poly[(*S*-B1)-*co*-(*S*-N2)]**, respectively. The mixed solution, at a final monomer concentration of 30 μM (i.e., 15 μM/monomer) was heated to 100 °C to reach the molecularly dissolved state and slowly cooled (0.3 °C min^{-1}) to 20 °C to perform the polymerization under thermodynamic control.

As visible by the naked eye, both mixtures form new aggregated states characterized by a blue-green emission for **poly[(*S*-B1)-*co*-(*S*-N2)** and a yellow emission for **poly[(*S*-B1)-*co*-(*S*-N1)]** (Figure 2a). Photoluminescence spectra of the two systems show the presence of a broad, featureless emission band for both **poly[(*S*-B1)-*co*-(*S*-N2)]** (λ_{em} = 520 nm) and **poly[(*S*-B1)-*co*-(*S*-N1)]** (λ_{em} = 550 nm) in addition to the emission of the homopolymers (Figure 2b). These red-shifted emission bands suggest the formation of B−N contacts in the form of excited-state complexes (exciplexes) (Figure 3a). By testing a set of different ***S*-B1**/***S*-N1** ratios, we observed that the exciplex band remains the predominant emission, even when decreasing ***S*-B1** down to 10 mol % of the total monomers' concentration (Figure S6).

To confirm the formation of B−N exciplexes in the supramolecular copolymers, we performed further photoluminescence experiments. Emission lifetime measurements indicate that the excited states attributed to these transitions exhibit two decay components (Figure 3b): one belonging to a species that has a fast decay, on the order of nanoseconds, and another to a long-lived species that fully decays on the order of microseconds (Figure S7). These results are in agreement with the hypothesis regarding the formation of B−N CT interactions (Figure 3a) as such long photoluminescence decays are often attributed to nonpermitted transitions such as CT complexes,[42] exciplexes,[43,44] and excited triplet states.[45] Further evidence that confirms the formation of B−N FLP is the presence of a weak CT absorption band (observed as a shoulder at $\lambda \sim$ 500 nm) in concentrated solutions of **poly[(*S*-B1)-*co*-(*S*-N1)]** in decalin (Figure S8), in line with previously reported B−N FLP couples.[41,46]

Because of spin statistics, CT processes give rise to both singlet and triplet excited states.[47,48] The triplet ground state of O_2 can interact with the triplet excited state of organic emitters and decay via different paths by which the emission of the organic molecules is quenched.[49−52] We thus compared the exciplex emissions obtained in degassed decalin with the

https://dx.doi.org/10.1021/jacs.0c06921
J. Am. Chem. Soc. 2020, 142, 16681−16689

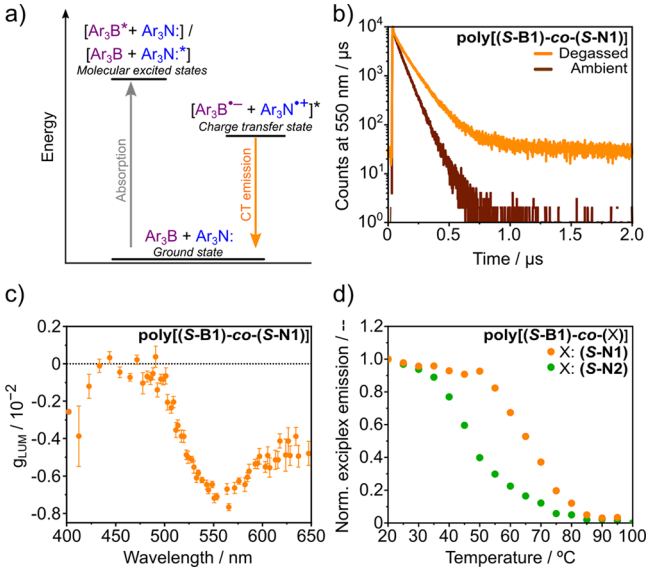

Figure 3. Photophysical study of B−N supramolecular copolymers. (a) Schematic representation of the mechanism of CT emission in the copolymers. Light absorption from the ground state converts each species to its molecular excited state, followed by CT with the ground state of another species. (b) Lifetime measurement of **poly**[(***S*-B1**)-*co*-(***S*-N1**)] for degassed (orange line) and air-equilibrated (brown line) decalin (λ_{em} = 550 nm, λ_{exc} = 400 nm, 20 °C). (c) Circularly polarized luminescence spectrum of **poly**[(***S*-B1**)-*co*-(***S*-N1**)] (λ_{exc} = 365 nm, 20 °C). (d) VT-photoluminescence cooling curves (λ_{ex} = 387 nm) for **poly**[(***S*-B1**)-*co*-(***S*-N2**)] (green dots; λ_{em} = 530 nm) and **poly**[(***S*-B1**)-*co*-(***S*-N1**)] (orange dots; λ_{em} = 600 nm).

samples prepared on the benchtop. As expected, O_2 significantly interferes with the photoluminescence as the intensity of exciplex emission is substantially higher in the absence of O_2 (Figure S9e). Furthermore, the absence of O_2 also strongly affects the lifetime of the excited states by increasing the lifetime of the long-lived species (Figure 3b for **poly**[(***S*-B1**)-*co*-(***S*-N1**)], Figure S10b for **poly**[(***S*-B1**)-*co*-(***S*-N2**)]). This indicates that the exciplexes of both copolymers operate via a thermally activated delayed fluorescence similarly to what has been previously observed in B−N-based OLED materials.[17,40]

The exciplex emission wavelength is an indicator of the energy of the CT interaction and can be correlated to the energetic difference between the donor's HOMO and the acceptor's LUMO. For both mixtures, the CT energy is relatively high (i.e., 2.2 eV for **poly**[(***S*-B1**)-*co*-(***S*-N1**)] and 2.4 eV for **poly**[(**S−B1**)-*co*-(**S−N2**)]), implying that the interaction between N and B is of a supramolecular nature.[17] Furthermore, the difference in energy observed between the two B−N mixtures highlights the formation of a stronger donor/acceptor complex in **poly**[(***S*-B1**)-*co*-(***S*-N1**)] than in **poly**[(***S*-B1**)-*co*-(***S*-N2**)]. This is rationalized by the different molecular structure of the monomers. The *O*-bridge of ***S*-N1** gives additional electron density to the core compared to that of ***S*-N2**, rendering ***S*-N1** a stronger electron donor.

Cofacial B−N pairs enchained within supramolecular copolymers can be distinguished from freely diffusing dimers in solution by measuring circularly polarized luminescence. We anticipated that enchained B−N FLPs would be sensitive to the chiral environment generated by the supramolecular copolymer and display anisotropy values for the exciplex emission (g_{LUM}) larger than the ones of simple dimers.[53,54] The measurement performed at 20 °C confirms this hypothesis for both exciplexes (Figure 3c and Figure S10c), showing g_{LUM} values on the order of 10^{-3}, which is typical for supramolecular assemblies.[55]

Further evaluation of the formation of the exciplex was performed by monitoring the evolution of the exciplex band as a function of temperature. To avoid the suppression of long-lived species, we carried out VT-photoluminescence measurements in degassed samples (Figure S11). The exciplex emissions of both **poly**[(***S*-B1**)-*co*-(***S*-N2**)] (Figure 3d, green dots, λ_{em} = 530 nm) and **poly**[(***S*-B1**)-*co*-(***S*-N1**)] (Figure 3d, orange dots, λ_{em} = 600 nm to eliminate the contribution of the homopolymers) start to emerge at ∼75 °C and follow a nonsigmoidal growth to a plateau (Figure 3d). Interestingly, 75 °C coincides with the T_e of **poly**(***S*-B1**) at 15 μM (*vide supra*) and with the copolymer's T_e observed by CD (*vide infra*), suggesting that the formation of both exciplexes begins with the elongation of the supramolecular aggregates.

Analysis of B−N Supramolecular Copolymerization. To further study the copolymerization, we complemented the photoluminescence studies with CD and UV−vis spectroscopy. As techniques that investigate the ground state of the systems instead of the excited state, CD and UV−vis are particularly useful for accessing details of the mechanism of copolymerization. Moreover, the combined analysis of the copolymerization cooling curves and the evaluation of the features of the copolymers' spectra gives information regarding the copolymers' microstructure. Interestingly, both CD and UV−vis measurements at 20 °C show the close resemblance of **poly**[(***S*-B1**)-*co*-(***S*-N2**)] spectra to the linear sum of the spectra of **poly**(***S*-B1**) and **poly**(***S*-N2**), which assumes no interaction between the two homopolymers (Figure 4a, Figure S12). Likewise, the CD cooling curve at 363 nm displays two independent transitions (75 and 45 °C) (Figure 4b, green line) and clearly matches the linear sum of the two homopolymers (Figure 4b, black line). As such, it is possible to correlate the two transitions of **poly**[(***S*-B1**)-*co*-(***S*-N2**)] to the T_e values for each homopolymer. Although at first glance these results suggest self-sorting between the two homopolymers, this hypothesis can be excluded on the basis of the photoluminescence study (*vide supra*).

The ten Eikelder/Markvoort mass balance model for copolymerization is a powerful tool for qualitatively rationalizing the copolymerization behavior and the microstructure by simulating hypothetical copolymerization scenarios.[9] To simulate a likely scenario for our systems, we selected the thermodynamic values of two hypothetical monomers, **A** and **B**, using the values calculated by fitting the cooling curves of **poly**(***S*-B1**) and **poly**(***S*-N2**), respectively. The enthalpy and entropy of heterointeraction were selected as the average of the homopolymerization values obtained by fitting. These initial settings give a cooling curve characterized by a double transition and demonstrates that the copolymerization can occur even when two transitions are detected. This is suggested by the average block lengths obtained for such simulated copolymer, which exhibits **A−B** bonds and an overall blocky structure (Figure 4c,d, Figure S13, Tables S1−S2).[56]

We further evaluated the copolymerization by performing a mixed sergeant-and-soldier experiment with ***S*-B1** and **a-N2**, the achiral analogue of ***S*-N2**. The achiral nature of **a-N2** renders **poly**(**a-N2**) racemic and, as a result, CD silent (Figure S14a). The CD spectrum of the resulting copolymer **poly**[(***S*-

https://dx.doi.org/10.1021/jacs.0c06921
J. Am. Chem. Soc. 2020, 142, 16681−16689

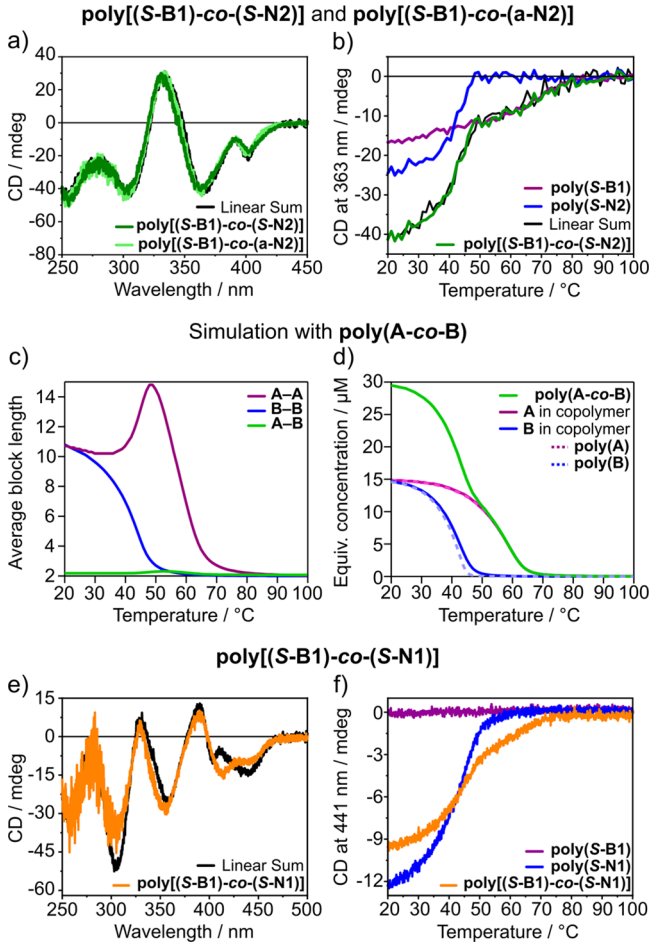

Figure 4. B–N supramolecular copolymerization. CD spectra at 20 °C of (a) **poly**[(***S*-B1**)-*co*-(***S*-N2**)] (dark green line) and **poly**[(***S*-B1**)-*co*-(**a-N2**)] (light green line), and of (e) **poly**[(***S*-B1**)-*co*-(***S*-N1**)] (orange line). Both systems are compared with the linear sum of the related homopolymers' CD spectra (black lines). (b) CD cooling curves of **poly**[(***S*-B1**)-*co*-(***S*-N2**)] (green line), poly(S–B1) (purple line), **poly**(***S*-N2**) (blue line), and the linear sum of the related homopolymers curves (black line). Simulation of hypothetical **poly**(**A**-*co*-**B**) showing (c) an average block length for homocontacts (**A–A**, purple line; **B–B**, blue line) and heterocontacts (**A–B**, green line) (an average block length of 2 is defined as a block containing 2 monomers and 1 bond); and (d) equivalent monomer concentrations in **poly**(**A**-*co*-**B**) (solid lines) and in the related homopolymers (dotted lines). (f) CD cooling curves of **poly**[(***S*-B1**)-*co*-(***S*-N1**)] (orange line), **poly**(***S*-B1**) (purple line), and **poly**(***S*-N1**) (blue line). Measurements were performed in decalin with each monomer at c = 15 μM and a cooling rate of 0.3 °C min^{-1}. The linear sum was calculated as [**poly**(***S*-B1**) + **poly**(***S*-N2**)] (and analogous for ***S*-N1**) with each monomer at c = 15 μM.

B1)-*co*-(**a-N2**)] closely resembles that of **poly**[(***S*-B1**)-*co*-(***S*-N2**)] (Figure 4a, light green line vs green line), showing the combined CD signatures of both boron and nitrogen aggregates. The result demonstrates that **poly**(***S*-B1**) transfers its helical bias to **poly**(**a-N2**), suggesting the copolymerization between ***S*-B1** and **a-N2** (Figure 4a, Figure S14b). Similar to **poly**[(***S*-B1**)-*co*-(***S*-N2**)], the CD cooling curve of **poly**[(***S*-B1**)-*co*-(**a-N2**)] also displays two transition temperatures corresponding to the homopolymers' T_e (Figure S14d). Since ***S*-N2** and **a-N2** differ only in their side chains and the copolymerization measurements closely resemble each other, we deduce that **poly**[(***S*-B1**)-*co*-(**a-N2**)] and **poly**[(***S*-B1**)-*co*-(***S*-N2**)] must, to a certain extent, have a similar copolymer microstructure.[9,56]

In contrast, the CD spectrum of **poly**[(***S*-B1**)-*co*-(***S*-N1**)] clearly deviates from the linear sum of [**poly**(***S*-B1**) + **poly**(***S*-N1**)] (Figure 4e, Figure S15a). Although it displays two transition temperatures, the CD cooling curve recorded at 412 nm significantly differs from the linear sum (Figure S15c). Because of the large difference between the spectroscopic signatures of **poly**(***S*-B1**) and **poly**(***S*-N1**), we were able to follow the copolymerization at a wavelength where only ***S*-N1** absorbs (λ_{CD} = 441 nm). The experiment confirms that the copolymerization of **poly**[(***S*-B1**)-*co*-(***S*-N1**)] starts at 75 °C (Figure 4f), as also shown by UV–vis (Figure S15d). In the absence of ***S*-B1**, **poly**(***S*-N1**) does not show helical order at temperatures higher than 50 °C (Figure 4f), while in the presence of ***S*-B1** we observe an initial growth in chiral structural order of ***S*-N1** aggregates in the 75–50 °C regime. We hence propose that, at 75 °C, ***S*-B1** nuclei serve as nucleation sites for a certain fraction of ***S*-N1** that, as a result, copolymerize with the nuclei. The second transition at 50 °C can then be attributed to the assembly of the remaining fraction of ***S*-N1** monomers.

Proposed Assembly Mode in Solution. For the interpretation of the copolymers microstructure, CD, UV–vis, and NMR (see discussion in Supporting Information and Figure S16) are techniques that measure the whole system, while photoluminescence measurements represent only the weighted average of emitting species based on their relative quantum yields. From CD studies we deduce that, between 75 and 50 °C (45 °C for ***S*-N2**), **poly**(***S*-B1**) is formed, while the majority of ***S*-N1** (or ***S*-N2**) is still molecularly dissolved (Figures 4b,f, 5). In this regime, a fraction of ***S*-N1** (or ***S*-N2**) is incorporated into the stack of **poly**(***S*-B1**), progressively creating B–N contacts that give rise to the exciplex emissions (Figure 3d, 5).Upon cooling below 50 °C (45 °C for ***S*-N2**), the remaining fraction of ***S*-N1** (or ***S*-N2**) copolymerizes onto the previously formed polymeric stacks (Figures 4c, 5) without significantly increasing the number of B–N contacts, as deduced from the flattening of the exciplex's cooling curves in the low-temperature regime (Figure 3d). At 20 °C, the circular polarization of the exciplex emission confirms the presence of a number of B–N contacts within the copolymers (*vide supra*), which is sufficient to dominate the emission profile of the system.[53,54] The coexistence of emission bands belonging to the homopolymers indicates the noncomplete mixing between B and N monomers, which is in-line with the temperature-dependent studies that point toward the formation of multiblock structures.

This description represents a general view of the copolymers; however, it is likely that the system forms a heterogeneous population of copolymers that do not have the same composition (i.e., block length and occurrence of each monomer in each chain)) but share similar microstructures (Figure 5, right). In solution, where the main driving force of assembly is due to H-bonding, the heterointeractions between ***S*-B1** and ***S*-N1** (or ***S*-N2**) compete against the homointeractions to define the final microstructure. We hypothesize that because of the relatively high electron density of the B core, which lowers its Lewis acidity,[57] the energy of interaction between the B and the N monomers is not sufficient to suppress the formation of homocontacts, thus resulting in a random blocklike structure rather than alternating B–N copolymers. Nonetheless, the number of heterocontacts is

https://dx.doi.org/10.1021/jacs.0c06921
J. Am. Chem. Soc. 2020, 142, 16681–16689

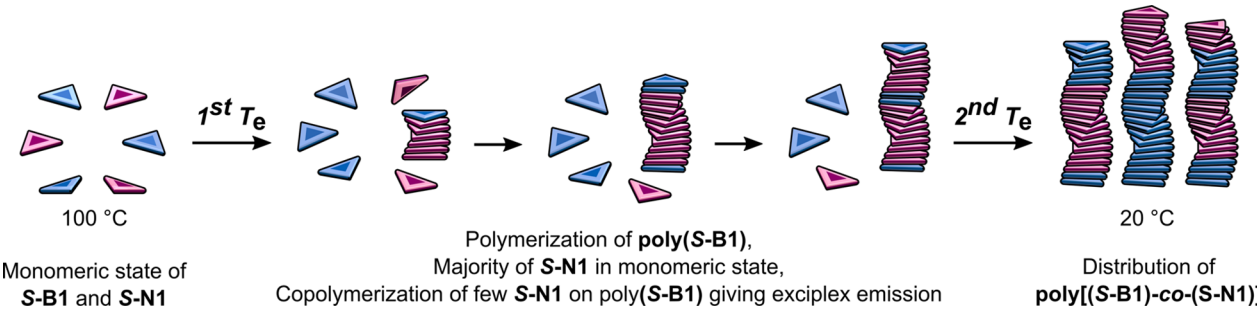

Figure 5. Proposed mechanism of copolymerization. Schematic representation of copolymerization via slow cooling from the monomerically dissolved state.

sufficient to generate intriguing emitting properties via B−N interactions, which we further investigated in bulk.

Bulk Properties of B−N Systems. Considering the possibility to increase the degree of mixing between B and N monomers by eliminating the thermodynamic variables associated with solvation, we further investigated the material properties in the bulk. We focused on **poly**[(***S*-B1**)-*co*-(***S*-N1**)], which forms the strongest donor/acceptor pair in this study (Figures 2 and 4e). Optical measurements were carried out on bulk films that were prepared by drop-casting a 1:1 ***S*-B1**/***S*-N1** solution from dichloromethane on a glass substrate and drying on a hot plate. As observed in solution (Figures 2a), the photoexcitation of **poly**[(***S*-B1**)-*co*-(***S*-N1**)] films with a long-wavelength UV lamp (365 nm) led to a yellow emission (λ_{em} = 550 nm), which clearly differs from the light blue emissions of the individual components (Figures 6a,b). The copolymers' exciplex emission band observed in bulk matches the one detected in solutions, indicating similar strengths of B−N interactions in both environments. However, the absence of the emission bands of homopolymers in the bulk suggests a higher degree of B−N mixing or a faster exciton migration in the solid state (Figure 6b) when compared to that in the copolymer in solutions. Similar to the solution-based measurements (Figure S8), B−N FLP interactions are also observed in the ground state, as indicated by the presence of a CT band at ∼500 nm in the UV−vis spectrum of the films (Figure S17).

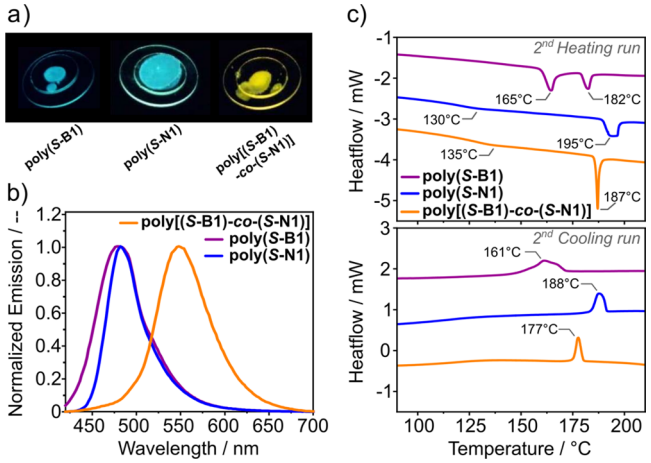

Figure 6. Bulk properties. (a) Picture of drop-casted samples under photoexcitation using a long-wavelength UV lamp and b) their photoluminescence emission spectra (λ_{exc} = 400 nm, 20 °C) **poly**(***S*-B1**) (purple line), **poly**(***S*-N1**) (blue line), and **poly**[(***S*-B1**)-*co*-(***S*-N1**)]) (orange line). (c) Heating (top) and cooling (bottom) DSC traces of **poly**(***S*-B1**), **poly**(***S*-N1**), and **poly**[(***S*-B1**)-*co*-(***S*-N1**)]. A second DSC run of the mixture prepared by dissolving both compounds in dichloromethane and drying on a DSC pan prior to the measurement. Cooling/heating rate = 10 °C min^{-1}, endothermic process is down.

The bulk material was then investigated by thermal and structural analysis. Differential scanning calorimetry (DSC) shows that **poly**(***S*-B1**) displays two phase transitions at 165 and 182 °C (Figure 6c, purple lines) in the second heating run and a single crystallization peak at 161 °C of the second cooling run. **Poly**(***S*-N1**) shows a broad glass transition at ∼130 °C and a melting peak at 195 °C (Figure 6c, blue lines), while its crystallization is detected at 188 °C in the cooling run. For **poly**[(***S*-B1**)-*co*-(***S*-N1**)], the characteristic peaks of the individual components are not found, while sharp melting and crystallization peaks are recorded at 187 and 177 °C, respectively (Figure 6c, orange lines; Figure S18c).

Nanoscale structures in bulk were characterized by polarized optical microscopy (Figure S19) and medium- and wide-angle X-ray scattering (Figure S20). At 20 °C, **poly**(***S*-B1**), **poly**(***S*-N1**), and the 1:1 mixture **poly**[(***S*-B1**)-*co*-(***S*-N1**)] show a hexagonally packed cylindrical phase with a domain spacing of 3.5 nm for **poly**(***S*-B1**) and 3.4 nm for **poly**(***S*-N1**) and **poly**[(***S*-B1**)-*co*-(***S*-N1**)], respectively. By preparation of the bulk material via slow cooling (5 °C min^{-1}), the scattering pattern of **poly**[(***S*-B1**)-*co*-(***S*-N1**)] follows that of **poly**(***S*-N1**), similar to what is observed in mixed liquid crystalline materials (Figure S20a).[58] In contrast, with fast cooling rates (20 °C min^{-1}), **poly**[(***S*-B1**)-*co*-(***S*-N1**)] shows a lamellar structure that completely deviates from the respective homopolymers (Figure S20b). This experiment confirms the formation of a mixed structure in the solid state and suggests that the presence of competitive interactions (e.g., H-bonding and B−N interaction) may result in the formation of different morphologies depending on the material processing methods, i.e., pathway complexity.

The difference in the mixing degree between solution and bulk measurement can be accounted by the competition between multiple noncovalent interactions. In both conditions, the competition between monomers' homointeractions and B−N heterointeractions defines the final nanostructure. However, the bulk lacks the additional solute−solvent interaction, which might be the main factor that reduces the B−N contacts in solution.

The results obtained from the bulk investigation are a good indication that the concept of supramolecular B−N copolymers can be optimized with the final aim to create alternating −B−N−B−N− arrays in highly ordered structures and represent an important step toward developing B−N functional materials. Moreover, the results are promising, such that

https://dx.doi.org/10.1021/jacs.0c06921
J. Am. Chem. Soc. 2020, 142, 16681−16689

these materials can possess interesting charge transport properties, which will be studied in due time.

CONCLUSIONS

In this work we reported the synthesis, assembly, and photophysical properties of triarylborane and triarylamine supramolecular homopolymers, with the aim to explore the role of frustrated Lewis pairs (FLP) in their copolymers. We introduced *O*-bridged triphenylborane and triarylamine cores and demonstrated their potential as appealing units for supramolecular optoelectronics by forming controlled chiral 1D supramolecular polymers. Studies on the copolymerization mechanism and microstructure indicate that B and N monomers act as true comonomers,[59] excluding the hypothesis of other interaction modes such as chain cappers or intercalator.[59] Supramolecular copolymers based on this pair display intriguing photoluminescence properties as a result of cofacial B−N contacts embedded in the chiral copolymers' structure. Upon excitation, this molecular arrangement facilitates the formation of an excited-state complex at the B−N interfaces, followed by circularly polarized emission. This exciplex emission also operates via a thermally activated delayed fluorescence mechanism with a lifetime of up to several microseconds.

To the best of our knowledge, the system reported here is the first example of circularly polarized exciplex emitters and the first demonstration of FLP-based supramolecular copolymers both in solution and in bulk. In addition to these unique observations, the study also generates several challenging questions that remain elusive because of the underlying complexity of the system. For instance, is it possible to form fully alternating structures with B−N pairs by increasing their Lewis acidity and basicity, respectively? Assuming so, how would the electronic communication between B and N comonomers be in a full stack? Fully conjugated or a stack of dimers? We aim to tackle these questions by increasing the hetero-interaction gain and play with the processing of these systems in bulk where promising results have already been observed. We anticipate that the interesting photophysical properties of B−N systems will be beneficial for future development of B−N materials in optoelectronic devices.

ASSOCIATED CONTENT

Supporting Information

The Supporting Information is available free of charge at https://pubs.acs.org/doi/10.1021/jacs.0c06921.

Experimental procedures, characterization data, details of theoretical modeling, and Figures S1−S20 (PDF)

AUTHOR INFORMATION

Corresponding Authors

E. W. Meijer − *Laboratory of Macromolecular and Organic Chemistry and Institute for Complex Molecular Systems, Department of Chemical Engineering and Chemistry, Eindhoven University of Technology, Eindhoven 5600 MB, The Netherlands;* orcid.org/0000-0003-4126-7492; Email: e.w.meijer@tue.nl

Shigehiro Yamaguchi − *Institute of Transformative Bio-Molecules (WPI-ITbM) and Department of Chemistry, Graduate School of Science and Integrated Research Consortium on Chemical Sciences (IRCCS), Nagoya University, Nagoya 464-8602, Japan;* orcid.org/0000-0003-0072-8969; Email: yamaguchi@chem.nagoya-u.ac.jp

Authors

Beatrice Adelizzi − *Laboratory of Macromolecular and Organic Chemistry and Institute for Complex Molecular Systems, Department of Chemical Engineering and Chemistry, Eindhoven University of Technology, Eindhoven 5600 MB, The Netherlands*

Pongphak Chidchob − *Laboratory of Macromolecular and Organic Chemistry and Institute for Complex Molecular Systems, Department of Chemical Engineering and Chemistry, Eindhoven University of Technology, Eindhoven 5600 MB, The Netherlands*

Naoki Tanaka − *Institute of Transformative Bio-Molecules (WPI-ITbM), Nagoya University, Nagoya 464-8602, Japan*

Brigitte A. G. Lamers − *Laboratory of Macromolecular and Organic Chemistry and Institute for Complex Molecular Systems, Department of Chemical Engineering and Chemistry, Eindhoven University of Technology, Eindhoven 5600 MB, The Netherlands*

Stefan C. J. Meskers − *Institute for Complex Molecular Systems, Department of Chemical Engineering and Chemistry, Eindhoven University of Technology, Eindhoven 5600 MB, The Netherlands;* orcid.org/0000-0001-9236-591X

Soichiro Ogi − *Department of Chemistry, Graduate School of Science and Integrated Research Consortium on Chemical Sciences (IRCCS), Nagoya University, Nagoya 464-8602, Japan*

Anja R. A. Palmans − *Laboratory of Macromolecular and Organic Chemistry and Institute for Complex Molecular Systems, Department of Chemical Engineering and Chemistry, Eindhoven University of Technology, Eindhoven 5600 MB, The Netherlands;* orcid.org/0000-0002-7201-1548

Complete contact information is available at: https://pubs.acs.org/10.1021/jacs.0c06921

Author Contributions

#B.A. and P.C. contributed equally to this work.

Notes

The authors declare no competing financial interest.

ACKNOWLEDGMENTS

The authors express their thanks to Prof. Dr. Shu Seki (Kyoto University), Dr. Nathan Van Zee, and Lafayette de Windt for fruitful discussions, Martin van Son for his support in film measurements, and Dr. Naoki Ando and Ms. Mika Sakai (Nagoya University) for their support in the synthesis of boron precursors. The work in The Netherlands received funding from The Netherlands Organization for Scientific Research (NWO-TOP PUNT Grant No. 10018944) and the Dutch Ministry of Education, Culture and Science (Gravitation Program 024.001.035). Beatrice Adelizzi received additional funding from the European Union's Horizon 2020 research and innovation program (SmartSAST Grant No. 890479). The work in Japan received funding from JSPS KAKENHI grants (18H03909 and 18H05261).

REFERENCES

(1) Frisch, H.; Fritz, E.-C.; Stricker, F.; Schmüser, L.; Spitzer, D.; Weidner, T.; Ravoo, B. J.; Besenius, P. Kinetically Controlled Sequential Growth of Surface-Grafted Chiral Supramolecular Copolymers. *Angew. Chem., Int. Ed.* **2016**, *55* (25), 7242−7246.

(2) Ressouche, E.; Pensec, S.; Isare, B.; Ducouret, G.; Bouteiller, L. Rational Design of Urea-Based Two-Component Organogelators. *ACS Macro Lett.* **2016**, *5* (2), 244−247.
(3) Yagai, S.; Hamamura, S.; Wang, H.; Stepanenko, V.; Seki, T.; Unoike, K.; Kikkawa, Y.; Karatsu, T.; Kitamura, A.; Würthner, F. Unconventional Hydrogen-Bond-Directed Hierarchical Co-Assembly between Perylene Bisimide and Azobenzene-Functionalized Melamine. *Org. Biomol. Chem.* **2009**, *7* (19), 3926−3929.
(4) Görl, D.; Zhang, X.; Stepanenko, V.; Würthner, F. Supramolecular Block Copolymers by Kinetically Controlled Co-Self-Assembly of Planar and Core-Twisted Perylene Bisimides. *Nat. Commun.* **2015**, *6* (1), 7009.
(5) Zhang, W.; Jin, W.; Fukushima, T.; Saeki, A.; Seki, S.; Aida, T. Supramolecular Linear Heterojunction Composed of Graphite-Like Semiconducting Nanotubular Segments. *Science* **2011**, *334* (6054), 340−343.
(6) Boott, C. E.; Leitao, E. M.; Hayward, D. W.; Laine, R. F.; Mahou, P.; Guerin, G.; Winnik, M. A.; Richardson, R. M.; Kaminski, C. F.; Whittell, G. R.; Manners, I. Probing the Growth Kinetics for the Formation of Uniform 1D Block Copolymer Nanoparticles by Living Crystallization-Driven Self-Assembly. *ACS Nano* **2018**, *12* (9), 8920−8933.
(7) Hudson, Z. M.; Lunn, D. J.; Winnik, M. A.; Manners, I. Colour-Tunable Fluorescent Multiblock Micelles. *Nat. Commun.* **2014**, *5* (1), 3372.
(8) Jung, S. H.; Bochicchio, D.; Pavan, G. M.; Takeuchi, M.; Sugiyasu, K. A Block Supramolecular Polymer and Its Kinetically Enhanced Stability. *J. Am. Chem. Soc.* **2018**, *140* (33), 10570−10577.
(9) Adelizzi, B.; Aloi, A.; Markvoort, A. J.; Ten Eikelder, H. M. M.; Voets, I. K.; Palmans, A. R. A.; Meijer, E. W. Supramolecular Block Copolymers under Thermodynamic Control. *J. Am. Chem. Soc.* **2018**, *140* (23), 7168−7175.
(10) Adelizzi, B.; Aloi, A.; Van Zee, N. J.; Palmans, A. R. A.; Meijer, E. W.; Voets, I. K. Painting Supramolecular Polymers in Organic Solvents by Super-Resolution Microscopy. *ACS Nano* **2018**, *12* (5), 4431−4439.
(11) Stephan, D. W. The Broadening Reach of Frustrated Lewis Pair Chemistry. *Science* **2016**, *354* (6317), aaf7229.
(12) Geier, S. J.; Gilbert, T. M.; Stephan, D. W. Activation of H2 by Phosphinoboranes R2PB(C6F5)2. *J. Am. Chem. Soc.* **2008**, *130* (38), 12632−12633.
(13) Meng, W.; Feng, X.; Du, H. Frustrated Lewis Pairs Catalyzed Asymmetric Metal-Free Hydrogenations and Hydrosilylations. *Acc. Chem. Res.* **2018**, *51* (1), 191−201.
(14) Paradies, J. Mechanisms in Frustrated Lewis Pair-Catalyzed Reactions. *Eur. J. Org. Chem.* **2019**, *2019* (2−3), 283−294.
(15) Chapman, A. M.; Haddow, M. F.; Wass, D. F. Frustrated Lewis Pairs beyond the Main Group: Synthesis, Reactivity, and Small Molecule Activation with Cationic Zirconocene−Phosphinoaryloxide Complexes. *J. Am. Chem. Soc.* **2011**, *133* (45), 18463−18478.
(16) Willms, A.; Schumacher, H.; Tabassum, T.; Qi, L.; Scott, S. L.; Hausoul, P. J. C.; Rose, M. Solid Molecular Frustrated Lewis Pairs in a Polyamine Organic Framework for the Catalytic Metal-Free Hydrogenation of Alkenes. *ChemCatChem* **2018**, *10* (8), 1835−1843.
(17) Goushi, K.; Yoshida, K.; Sato, K.; Adachi, C. Organic Light-Emitting Diodes Employing Efficient Reverse Intersystem Crossing for Triplet-to-Singlet State Conversion. *Nat. Photonics* **2012**, *6* (4), 253−258.
(18) Ye, T.; Chen, W.; Jin, S.; Hao, S.; Zhang, X.; Liu, H.; He, D. Enhanced Efficiency of Planar Heterojunction Perovskite Solar Cells by a Light Soaking Treatment on Tris(Pentafluorophenyl)Borane-Doped Poly(Triarylamine) Solution. *ACS Appl. Mater. Interfaces* **2019**, *11* (15), 14004−14010.
(19) Gao, F.-W.; Zhang, F.-Y.; Zhong, R.-L.; Xu, H.-L.; Sun, S.-L.; Su, Z.-M. Boron/Nitrogen Substituted the Staggered Hetero-Dimers: Fascinating Intermolecular Charge-Transfer and Large NLO Responses. *Dyes Pigm.* **2017**, *145*, 21−28.
(20) Wang, M.; Nudelman, F.; Matthes, R. R.; Shaver, M. P. Frustrated Lewis Pair Polymers as Responsive Self-Healing Gels. *J. Am. Chem. Soc.* **2017**, *139* (40), 14232−14236.
(21) Chen, L.; Liu, R.; Yan, Q. Polymer Meets Frustrated Lewis Pair: Second-Generation CO2-Responsive Nanosystem for Sustainable CO2 Conversion. *Angew. Chem., Int. Ed.* **2018**, *57* (30), 9336−9340.
(22) Yokoyama, D. Molecular Orientation in Small-Molecule Organic Light-Emitting Diodes. *J. Mater. Chem.* **2011**, *21* (48), 19187−19202.
(23) Sakurai, T.; Yoneda, S.; Sakaguchi, S.; Kato, K.; Takata, M.; Seki, S. Donor/Acceptor Segregated π-Stacking Arrays by Use of Shish-Kebab-Type Polymeric Backbones: Highly Conductive Discotic Blends of Phthalocyaninatopolysiloxanes and Perylenediimides. *Macromolecules* **2017**, *50* (23), 9265−9275.
(24) Adelizzi, B.; Filot, I. A. W.; Palmans, A. R. A.; Meijer, E. W. Unravelling the Pathway Complexity in Conformationally Flexible N-Centered Triarylamine Trisamides. *Chem. - Eur. J.* **2017**, *23* (25), 6103−6110.
(25) Van Zee, N. J.; Adelizzi, B.; Mabesoone, M. F. J.; Meng, X.; Aloi, A.; Zha, R. H.; Lutz, M.; Filot, I. A. W.; Palmans, A. R. A.; Meijer, E. W. Potential Enthalpic Energy of Water in Oils Exploited to Control Supramolecular Structure. *Nature* **2018**, *558* (7708), 100−103.
(26) Kushida, T.; Shuto, A.; Yoshio, M.; Kato, T.; Yamaguchi, S. A Planarized Triphenylborane Mesogen: Discotic Liquid Crystals with Ambipolar Charge-Carrier Transport Properties. *Angew. Chem., Int. Ed.* **2015**, *54* (23), 6922−6925.
(27) Kushida, T.; Camacho, C.; Shuto, A.; Irle, S.; Muramatsu, M.; Katayama, T.; Ito, S.; Nagasawa, Y.; Miyasaka, H.; Sakuda, E.; Kitamura, N.; Zhou, Z.; Wakamiya, A.; Yamaguchi, S. Constraint-Induced Structural Deformation of Planarized Triphenylboranes in the Excited State. *Chem. Sci.* **2014**, *5* (4), 1296−1304.
(28) Martín, N. Tetrathiafulvalene: The Advent of Organic Metals. *Chem. Commun.* **2013**, *49* (63), 7025−7027.
(29) Lorbach, A.; Hübner, A.; Wagner, M. Aryl(Hydro)Boranes: Versatile Building Blocks for Boron-Doped π-Electron Materials. *Dalt. Trans.* **2012**, *41* (20), 6048−6063.
(30) Zhou, Z.; Wakamiya, A.; Kushida, T.; Yamaguchi, S. Planarized Triarylboranes: Stabilization by Structural Constraint and Their Plane-to-Bowl Conversion. *J. Am. Chem. Soc.* **2012**, *134* (10), 4529−4532.
(31) Nishimura, H.; Hasegawa, Y.; Wakamiya, A.; Murata, Y. Development of Transparent Organic Hole-Transporting Materials Using Partially Oxygen-Bridged Triphenylamine Skeletons. *Chem. Lett.* **2017**, *46* (6), 817−820.
(32) Moulin, E.; Armao, J. J.; Giuseppone, N. Triarylamine-Based Supramolecular Polymers: Structures, Dynamics, and Functions. *Acc. Chem. Res.* **2019**, *52* (4), 975−983.
(33) Haedler, A. T.; Kreger, K.; Issac, A.; Wittmann, B.; Kivala, M.; Hammer, N.; Köhler, J.; Schmidt, H.-W.; Hildner, R. Long-Range Energy Transport in Single Supramolecular Nanofibres at Room Temperature. *Nature* **2015**, *523* (7559), 196−199.
(34) Dorca, Y.; Naranjo, C.; Ghosh, G.; Gómez, R.; Fernández, G.; Sánchez, L. Unconventional Chiral Amplification in Luminescent Supramolecular Polymers Based on Trisbiphenylamine-Tricarboxamides. *Org. Mater.* **2020**, *02* (01), 041−046.
(35) Hirai, H.; Nakajima, K.; Nakatsuka, S.; Shiren, K.; Ni, J.; Nomura, S.; Ikuta, T.; Hatakeyama, T. One-Step Borylation of 1,3-Diaryloxybenzenes Towards Efficient Materials for Organic Light-Emitting Diodes. *Angew. Chem., Int. Ed.* **2015**, *54* (46), 13581−13585.
(36) Wakamiya, A.; Nishimura, H.; Fukushima, T.; Suzuki, F.; Saeki, A.; Seki, S.; Osaka, I.; Sasamori, T.; Murata, M.; Murata, Y.; Kaji, H. On-Top π-Stacking of Quasiplanar Molecules in Hole-Transporting Materials: Inducing Anisotropic Carrier Mobility in Amorphous Films. *Angew. Chem., Int. Ed.* **2014**, *53* (23), 5800−5804.
(37) Kitamoto, Y.; Suzuki, T.; Miyata, Y.; Kita, H.; Funaki, K.; Oi, S. The First Synthesis and X-Ray Crystallographic Analysis of an

https://dx.doi.org/10.1021/jacs.0c06921
J. Am. Chem. Soc. 2020, 142, 16681−16689

Oxygen-Bridged Planarized Triphenylborane. *Chem. Commun.* **2016**, *52* (44), 7098−7101.
(38) Hunter, C. A.; Sanders, J. K. M. The Nature of.Pi.-.Pi. Interactions. *J. Am. Chem. Soc.* **1990**, *112* (14), 5525−5534.
(39) Hunter, C. A.; Lawson, K. R.; Perkins, J.; Urch, C. J. Aromatic Interactions. *J. Chem. Soc. Perkin Trans. 2* **2001**, *5*, 651−669.
(40) Sarma, M.; Wong, K.-T. Exciplex: An Intermolecular Charge-Transfer Approach for TADF. *ACS Appl. Mater. Interfaces* **2018**, *10* (23), 19279−19304.
(41) Holtrop, F.; Jupp, A.; van Leest, K.; Paradiz Dominguez, M.; Williams, R.; Brouwer, F.; de Bruin, B.; Ehlers, A.; Slootweg, C. Photoinduced and Thermal Single-Electron Transfer to Generate Radicals from Frustrated Lewis Pairs. *Chem. - Eur. J.* **2020**, *26* (41), 9005−9011.
(42) Verhoeven, J. W. On the Role of Spin Correlation in the Formation, Decay, and Detection of Long-Lived, Intramolecular Charge-Transfer States. *J. Photochem. Photobiol., C* **2006**, *7* (1), 40−60.
(43) Shih, C.-J.; Lee, C.-C.; Yeh, T.-H.; Biring, S.; Kesavan, K. K.; Amin, N. R. A.; Chen, M.-H.; Tang, W.-C.; Liu, S.-W.; Wong, K.-T. Versatile Exciplex-Forming Co-Host for Improving Efficiency and Lifetime of Fluorescent and Phosphorescent Organic Light-Emitting Diodes. *ACS Appl. Mater. Interfaces* **2018**, *10* (28), 24090−24098.
(44) Dimitriev, O. P.; Piryatinski, Y. P.; Slominskii, Y. L. Excimer Emission in J-Aggregates. *J. Phys. Chem. Lett.* **2018**, *9* (9), 2138−2143.
(45) Hoffmann, S. T.; Schrögel, P.; Rothmann, M.; Albuquerque, R. Q.; Strohriegl, P.; Köhler, A. Triplet Excimer Emission in a Series of 4,4′-Bis(N-Carbazolyl)-2,2′-Biphenyl Derivatives. *J. Phys. Chem. B* **2011**, *115* (3), 414−421.
(46) Aramaki, Y.; Imaizumi, N.; Hotta, M.; Kumagai, J.; Ooi, T. Exploiting Single-Electron Transfer in Lewis Pairs for Catalytic Bond-Forming Reactions. *Chem. Sci.* **2020**, *11* (17), 4305−4311.
(47) Armstrong, N. R.; Wightman, R. M.; Gross, E. M. Light-Emitting Electrochemical Processes. *Annu. Rev. Phys. Chem.* **2001**, *52* (1), 391−422.
(48) Tao, Y.; Yuan, K.; Chen, T.; Xu, P.; Li, H.; Chen, R.; Zheng, C.; Zhang, L.; Huang, W. Thermally Activated Delayed Fluorescence Materials Towards the Breakthrough of Organoelectronics. *Adv. Mater.* **2014**, *26* (47), 7931−7958.
(49) Ware, W. R. Oxygen Quenching of Fluorescece in Solution: An Experimental Study of the Diffusion Process. *J. Phys. Chem.* **1962**, *66* (3), 455−458.
(50) Gijzeman, O. L. J.; Kaufman, F.; Porter, G. Oxygen Quenching of Aromatic Triplet States in Solution. Part 1. *J. Chem. Soc., Faraday Trans. 2* **1973**, *69* (0), 708−720.
(51) Gorman, A. A.; Rodgers, M. A. J. The Quenching of Aromatic Ketone Triplets by Oxygen: Competing Singlet Oxygen and Biradical Formation? *J. Am. Chem. Soc.* **1986**, *108* (17), 5074−5078.
(52) Nau, W. M.; Scaiano, J. C. Oxygen Quenching of Excited Aliphatic Ketones and Diketones. *J. Phys. Chem.* **1996**, *100* (27), 11360−11367.
(53) Han, J.; Guo, S.; Lu, H.; Liu, S.; Zhao, Q.; Huang, W. Recent Progress on Circularly Polarized Luminescent Materials for Organic Optoelectronic Devices. *Adv. Opt. Mater.* **2018**, *6* (17), 1800538.
(54) Sang, Y.; Han, J.; Zhao, T.; Duan, P.; Liu, M. Circularly Polarized Luminescence in Nanoassemblies: Generation, Amplification, and Application. *Adv. Mater.* **2019**, 1900110.
(55) Sánchez-Carnerero, E. M.; Agarrabeitia, A. R.; Moreno, F.; Maroto, B. L.; Muller, G.; Ortiz, M. J.; de la Moya, S. Circularly Polarized Luminescence from Simple Organic Molecules. *Chem. - Eur. J.* **2015**, *21* (39), 13488−13500.
(56) ten Eikelder, H. M. M.; Adelizzi, B.; Palmans, A. R. A.; Markvoort, A. J. Equilibrium Model for Supramolecular Copolymerizations. *J. Phys. Chem. B* **2019**, *123* (30), 6627−6642.
(57) Kitamoto, Y.; Kobayashi, F.; Suzuki, T.; Miyata, Y.; Kita, H.; Funaki, K.; Oi, S. Investigation of the Lewis Acidic Behaviour of an Oxygen-Bridged Planarized Triphenylborane toward Amines and the Properties of Their Lewis Acid-Base Adducts. *Dalt. Trans.* **2019**, *48* (6), 2118−2127.
(58) Yano, K.; Itoh, Y.; Araoka, F.; Watanabe, G.; Hikima, T.; Aida, T. Nematic-to-Columnar Mesophase Transition by in Situ Supramolecular Polymerization. *Science* **2019**, *363* (6423), 161−165.
(59) Weyandt, E.; Mabesoone, M. F. J.; de Windt, L. N. J.; Meijer, E. W.; Palmans, A. R. A.; Vantomme, G. How to Determine the Role of an Additive on the Length of Supramolecular Polymers? *Org. Mater.* **2020**, *02* (02), 129−142.

https://dx.doi.org/10.1021/jacs.0c06921
J. Am. Chem. Soc. 2020, 142, 16681−16689